Journal of Sound and Vibration (2001) **244**(3), 431–451
doi:10.1006/jsvi.2000.3473, available online at http://www.idealibrary.com on IDEAL®

MODAL UNCOUPLING OF DAMPED GYROSCOPIC SYSTEMS

J. T. Sawicki

Department of Mechanical Engineering, Cleveland State University, Cleveland, OH 44115-2425, *U.S.A.*
E-mail: j.sawicki@csuohio.edu

AND

G. Genta

Department of Mechanics, Politecnico di Torino, Corso Duca degli Abruzzi 24, 10129 *Torino, Italy.*
E-mail: genta@polito.it

(*Received* 3 *May* 2000, *and in final form* 1 *September* 2000)

A new approach for uncoupling the equations of motion typical for rotordynamical systems is presented. The method does not neglect the speed-dependent effects, such as gyroscopic effects, and can be particularly valuable in the controller design of actively controlled rotors. In the presence of hysteretic type of damping, the resulting uncoupled gyroscopic systems come with an equivalent viscous damping, equivalent in a sense of yielding the same natural frequency and decay rate. The approach is illustrated through three examples of technical interest: a Jeffcott rotor with hysteretic damping, a Stodola–Green rotor, and a rotor of a small gas turbine. The generated results demonstrate that the developed approach is correct and straightforward.

1. INTRODUCTION

The dynamic behaviour of rotors (mainly their natural frequencies and the corresponding mode shapes) can be strongly influenced by the spin speed. Apart from the speed-dependent characteristics of the bearings, the causes intrinsically linked with the rotor itself are mainly four: gyroscopic effect, rotating damping, centrifugal stiffening and deviation from axial symmetry [1]. While rotating damping has a very small effect on the natural frequencies of the system (it may have a very strong effect on the decay rate, to the point of making the system unstable), and centrifugal stiffening is usually important only for the natural frequencies linked with the blades of bladed rotors, gyroscopic effect has a deep influence on the dynamic behaviour of a large class of rotors. Generally speaking, it is owing to the gyroscopic effect that the Campbell diagram of most rotating machines is not ‘flat” like that of the Jeffcott rotor.

The importance of taking into account gyroscopic effect when modelling rotors is well understood, and most codes used to compute the critical speeds, the unbalance response and the Campbell diagram of rotors take it into account, introducing a suitable gyroscopic matrix into the equation of motion. Depending on the approach used for the discretization of the system, such a matrix may be a “lumped” one, when discrete discs with their polar and transverse moments of inertia are included at some locations, or a “consistent” one, when using the finite element method to derive the mass and gyroscopic matrices.

However, there are cases, mainly in the design of controllers for actively controlled rotors, in which the dynamics of the system is studied neglecting the spin speed, in the hope that the

0022-460X/01/280431 + 21 $35.00/0

effects of rotation, and hence also gyroscopic effect, can be included in the unmodelled or parasitic dynamics of the system without resulting in large errors. Moreover, there are cases in which reduced order models based on modal co-ordinates are used. These models are based on modal uncoupling and take into account only a small, often very small, number of modes, without taking into account that gyroscopic effect couples the various modes. If the rotor can be considered a weakly gyroscopic system, the result is an approximation not dissimilar to that due to neglecting the modal coupling caused by damping, centrifugal stiffening, non-linearities, etc., but this is not generally the case and larger errors can be expected.

It must also be noted that, if the inertial characteristics of the rotor are such that the polar (J_p) and transverse (diametral) (J_t) moments of inertia are approximately equal, the critical speeds computed without taking into account gyroscopic moments are little affected by it. However, even in this case, the Campbell diagram is not flat and new, very dangerous, critical speeds may appear in the supercritical region. Very large unbalance responses, not predicted by the reduced model, and shifts of the natural frequencies can appear.

The purpose of this paper is to introduce an uncoupling of the equations of motion which does not neglect the speed-depending effects, like a gyroscopic effect, particularly for the application to the design of the controller of actively controlled machines.

2. ROTOR EQUATION OF MOTION

Consider a multi-degree-of-freedom linear system made of an isotropic rotor running on a general stator. Its equation of motion can be written with reference to real or to complex co-ordinates [1, 2]. In the latter case, the gyroscopic matrix is symmetric, while in the former one it is skew symmetric. Using the real co-ordinates approach, the equation of motion is

$$\mathbf{M}\ddot{\mathbf{x}} + (\mathbf{C} + \omega\mathbf{G})\dot{\mathbf{x}} + (\mathbf{K} + \omega\mathbf{C}_r + \mathbf{K}_\omega\omega^2)\,\mathbf{x} = \mathbf{f}_n(t) + \omega^2\,\mathbf{f}_r(t), \tag{1}$$

where the mass $\mathbf{M}$, damping $\mathbf{C}$ (total, rotating plus non-rotating), stiffness $\mathbf{K}$ and centrifugal stiffening $\mathbf{K}_\omega$ matrices are symmetrical and independent from the spin speed, except for the case of the matrices coming from the linearization of hydrodynamic bearings (8-coefficients models) while the gyroscopic $\mathbf{G}$ and the circulatory (rotating damping) $\mathbf{C}_r$ matrices are skew symmetric; the non-rotating force vector $\mathbf{f}_n(t)$ is a generic function of time while the rotating force vector $\mathbf{f}_r(t)$ due to unbalance is a harmonic function of time with a period corresponding to the rotation frequency.

For the study of the lateral dynamics, it may be expedient to write separately the contributions in the two inflection planes xz and yz (z-axis has been assumed to be the axis of rotation) by reordering the generalized co-ordinates, with those related to the xz plane before those related to the yz plane:

$$\begin{bmatrix} \mathbf{M}_x & \mathbf{M}_{xy} \\ \mathbf{M}_{yx} & \mathbf{M}_y \end{bmatrix} \ddot{\mathbf{x}} + \left(\omega \begin{bmatrix} 0 & \mathbf{G}_{xy} \\ -\mathbf{G}_{yx} & 0 \end{bmatrix} + \begin{bmatrix} C_x & C_{xy} \\ C_{yx} & C_y \end{bmatrix} \right) \dot{\mathbf{x}}$$
$$+ \left(\begin{bmatrix} (\mathbf{K} + \mathbf{K}_\omega\omega^2)_x & (\mathbf{K} + \mathbf{K}_\omega\omega^2)_{xy} \\ (\mathbf{K} + \mathbf{K}_\omega\omega^2)_{yx} & (\mathbf{K} + \mathbf{K}_\omega\omega^2)_y \end{bmatrix} + \omega \begin{bmatrix} \mathbf{0} & \mathbf{C}_{r_{xy}} \\ -\mathbf{C}_{r_{yx}} & 0 \end{bmatrix} \right) \mathbf{x} = \mathbf{f}_n(t) + \omega^2 \mathbf{f}_r(t), \tag{2}$$

where the gyroscopic $\mathbf{G}_{ij}$ and the circulatory $\mathbf{C}_{r_{ij}}$ matrices are different from those in equation (1) and are symmetrical. Moreover, if the lumped parameters approach is used, matrices $\mathbf{G}$ are diagonal and their elements vanish in correspondence to the translational

degrees of freedom and are equal to the polar moment of inertia J_p associated with the nodes for rotational degrees of freedom.

Equation (2) can be expressed in modal co-ordinates in the form

$$\ddot{\boldsymbol{\eta}} + (\bar{\mathbf{C}} + \omega\bar{\mathbf{G}})\,\dot{\boldsymbol{\eta}} + (\bar{\mathbf{K}} + \omega\bar{\mathbf{C}}_r + \bar{\mathbf{K}}_\omega\omega^2)\,\boldsymbol{\eta} = \bar{\mathbf{f}}_n(t) + \omega^2\,\bar{\mathbf{f}}_r(t), \tag{3}$$

where the modal co-ordinates η_i are referred to the eigenvectors of the undamped, non-rotating system, normalized in such a way that the mass matrix is an identity matrix. The modal stiffness matrix is then diagonal and its elements are the squares of the natural frequencies of the undamped, non-rotating system. All other matrices are not diagonal and couple all modes. It is possible to define a proportional damping and a proportional centrifugal stiffness matrix in such a way that the corresponding modal matrices are diagonal and do not couple equation (3). The gyroscopic and circulatory matrices always couple the equations, but in the case of axisymmetrical systems, it is also possible to define a proportional form in which the equations uncouple in pairs, each pair being referred to two modes in the two inflection planes with the same frequency. In this case, very simple models can be devised by introducing the complex co-ordinates $z = x + \mathrm{i}y$ for translational degrees of freedom and $\phi = \phi_y - \mathrm{i}\phi_x$ for rotational ones. Note that while complex co-ordinates can greatly simplify the equation of motion of axisymmetrical systems, they can be used also in the study of general, non-isotropic, rotating systems.

When using the complex-co-ordinates notation, the equation of motion of an axisymmetrical rotating system is

$$\mathbf{M}\ddot{\mathbf{q}} + (\mathbf{C} - \mathrm{i}\omega\mathbf{G})\,\dot{\mathbf{q}} + (\mathbf{K} + \mathbf{K}_\omega\omega^2 - \mathrm{i}\omega\mathbf{C}_r)\,\mathbf{q} = \mathbf{f}_n(t) + \omega^2\,\mathbf{f}_r\,\mathrm{e}^{\mathrm{i}\omega t}. \tag{4}$$

The matrices which are symmetric when using the real co-ordinates approach are real in the equation written in terms of complex co-ordinates, while skew-symmetric matrices give way to symmetric, imaginary terms. When using the complex co-ordinates approach, all relevant matrices are then symmetric.

Also in this case there is no difficulty in performing a modal transformation using the eigenvector of the undamped non-rotating system

$$\ddot{\boldsymbol{\eta}} + (\bar{\mathbf{C}} - \mathrm{i}\omega\bar{\mathbf{G}})\,\dot{\boldsymbol{\eta}} + (\bar{\mathbf{K}} + \bar{\mathbf{K}}_\omega\omega^2 - \mathrm{i}\omega\bar{\mathbf{C}}_r)\,\boldsymbol{\eta} = \bar{\mathbf{f}}_n(t) + \omega^2\,\bar{\mathbf{f}}_r\,\mathrm{e}^{\mathrm{i}\omega t}, \tag{5}$$

where the only matrix to be diagonal is $\bar{\mathbf{K}}$. Clearly, the symmetric but non-diagonal matrices $\bar{\mathbf{C}}$, $\bar{\mathbf{G}}$, $\bar{\mathbf{K}}_\omega$ and $\mathbf{C}_r$ couple the equations of motion. Again, in the case of weakly damped and gyroscopic systems, also with a weak centrifugal stiffening effect, the terms outside the main diagonal of such matrices may be neglected and the equations of motion may be uncoupled in an approximated way, as already seen for the case in which real co-ordinates are used.

3. UNCOUPLING OF THE EQUATIONS IN THE STATE SPACE

The uncoupling of gyroscopic systems, in the context of rotor dynamics, can be performed in several ways; see for example references [3–5]. Genta [6] proposed to split the fully populated modal damping and gyroscopic matrices into the proportional (diagonal) and non-proportional part (off-diagonal elements). If the latter is negligible, modal uncoupling can be performed and the computation of the Campbell diagram becomes very easy. In the other case, a fast converging iterative procedure was proposed. The estimation of the errors associated with neglecting the coupling between the normal modes for non-gyroscopic systems can be found in reference [7]. Recently, Wang and Kirkhope [8, 9] showed that a set of real eigenvectors exists which constructs a basis for the vector space of systems with only gyroscopic coupling. The original complex eigenvalue problem can be

transformed into a real one in terms of two real symmetric matrices composed of the original mass, gyroscopic and stiffness matrices, and a closed-form response can be derived.

By writing the equation of motion (4) with reference to the complex state space, the usual equation

$$\dot{\mathbf{z}} = \mathbf{A}\mathbf{z} + \mathbf{B}\mathbf{u} \tag{6}$$

is obtained, where the state vector $\mathbf{z}$ and the dynamic matrix $\mathbf{A}$ are

$$\mathbf{z} = \begin{Bmatrix} \dot{\mathbf{q}} \\ \mathbf{q} \end{Bmatrix}, \quad \mathbf{A} = \begin{bmatrix} -\mathbf{M}^{-1}(\mathbf{C} - \mathrm{i}\omega\mathbf{G}) & -\mathbf{M}^{-1}(\mathbf{K} + \mathbf{K}_\omega \omega^2 - \mathrm{i}\omega\mathbf{C}_r) \\ \mathbf{I} & \mathbf{0} \end{bmatrix}. \tag{7}$$

Note that the dynamic matrix is complex, even in the case of undamped systems. Its eigenvalues are then complex but not conjugate: this physically means that the whirl frequencies of forward modes do not coincide with those of the backward modes.

The input gain matrix can have different expressions. As an example, in the case of the unbalance forces it is possible to consider a single input proportional to the square of the spin speed, obtaining

$$\mathbf{B}_u = \begin{bmatrix} \mathbf{M}^{-1}\mathbf{f}_r \\ \mathbf{0} \end{bmatrix}, \quad \mathbf{u}_u = \omega^2 \, \mathrm{e}^{\mathrm{i}\omega t}. \tag{8}$$

If the non-rotating forces $\mathbf{f}_n$ act on a number of stations of the rotor, the input gain matrix and the input vector can be written as

$$\mathbf{B}_n = \begin{bmatrix} \mathbf{M}^{-1}\mathbf{T}_n \\ \mathbf{0} \end{bmatrix}, \quad \mathbf{u}_n = \mathbf{f}_n, \tag{9}$$

where $\mathbf{T}_n$ is a selection matrix which identifies the degrees of freedom to which the generalized forces are applied. The same relationship applies for the control forces in the case of a controlled rotor.

It is well known that if the matrix $\mathbf{U}$ of the complex right eigenvectors of the dynamic matric $\mathbf{A}$ is obtained, it is possible to uncouple the equations of motion in the form

$$\dot{\bar{\mathbf{z}}} = \mathbf{U}^{-1}\mathbf{A}\mathbf{U}\bar{\mathbf{z}} + \mathbf{U}^{-1}\mathbf{B}\mathbf{u}, \tag{10}$$

where modal dynamic matrix $\bar{\mathbf{A}} = \mathbf{U}^{-1}\mathbf{A}\mathbf{U}$ is a complex diagonal matrix and $\bar{\mathbf{z}} = \mathbf{U}^{-1}\mathbf{z}$ are the modal states of the system. Equation (10) is a set of $2n$ uncoupled equations, if the number of complex degrees of freedom is n. Note that this uncoupling can be performed also in the case of a damped gyroscopic system; however, it requires the modal dynamic matrix and the modal input gain matrix for each value of the spin speed ω to be recalculated. This implies the solution of an eigenproblem of order $2n$ for each value of the speed, which is, however, exactly what is needed for plotting the Campbell diagram.

In the case of an undamped gyroscopic system the eigenvalues of the dynamic matrix $\mathbf{A}$ are imaginary and the eigenvectors have the first n elements which are imaginary and the other ones which are real.

While equation (10) is all that is needed for uncoupling the equations of motion (written with reference to the state space) of any damped gyroscopic system, a further elaboration intended to obtain uncoupled equations in the configuration space (i.e., aimed to split the multi-degrees-of-freedom rotor into a number of uncoupled single-degree of freedom rotors) may be useful. If the eigenvalues are ordered in such a way that the forward–backward pairs are placed one after the other, the system with n complex degrees of freedom can be split into n gyroscopic systems with a single degree of freedom, whose equations of motion are

$$\ddot{\eta}_i + (\bar{C}_i - \mathrm{i}\omega\bar{G}_i)\,\dot{\eta}_i + (\bar{K}_i - \mathrm{i}\omega\bar{C}_{ri})\,\eta_i = \bar{f}_{n_i}(t) + \omega^2 \bar{f}_{r_i} \, \mathrm{e}^{\mathrm{i}\omega t}. \tag{11}$$

The modal parameters can be easily computed by solving the eigenproblem related to the homogeneous equation (11) and equating the solution to the ith pair of eigenvalues (s_{i+} and s_{i-}, where the signs + and − identify the forward and backward modes) of the original system

$$\begin{bmatrix} 1 & \omega\Im(s_{i-}) & \Re(s_{i-}) & 0 \\ 0 & -\omega\Re(s_{i-}) & \Im(s_{i-}) & -\omega \\ 1 & \omega\Im(s_{i+}) & \Re(s_{i+}) & 0 \\ 0 & -\omega\Re(s_{i+}) & \Im(s_{i+}) & -\omega \end{bmatrix} \begin{Bmatrix} \bar{K}_1 \\ \bar{G}_i \\ \bar{C}_i \\ \bar{C}_{ri} \end{Bmatrix} = \begin{Bmatrix} \Im(s_{i-})^2 - \Re(s_{i-})^2 \\ -2\Im(s_{i-})\,\Re(s_{i-}) \\ \Im(s_{i+})^2 - \Re(s_{i+})^2 \\ -2\Im(s_{i+})\,\Re(s_{i+}) \end{Bmatrix}. \tag{12}$$

Equation (12) is easily solved in a closed form, yielding

$$\begin{aligned} \bar{K}_i &= -\Im(s_{i-})\,\Im(s_{i+}) + \Re(s_{i-})\,\Re(s_{i+}), \\ \bar{G}_i &= \tfrac{1}{\omega}[\Im(s_{i-}) + \Im(s_{i+})], \\ \bar{C}_i &= -\Re(s_{i-}) - \Re(s_{i+}), \\ \bar{C}_{ri} &= -\tfrac{1}{\omega}[\Re(s_{i-})\,\Im(s_{i-}) + \Re(s_{i+})\,\Im(s_{i+})]. \end{aligned} \tag{13}$$

Note that by definition $\Im(s_{i+})$ is positive while $\Im(s_{i-})$, is negative. In the case of the undamped system, the eigenvalues are imaginary and $\bar{K}_i = -\Im(s_{i-})\,\Im(s_{i+})$.

The modal parameters of the system can thus be used to write a state-space equation

$$\dot{\bar{\mathbf{z}}} = \bar{\mathbf{A}}\bar{\mathbf{z}} + \bar{\mathbf{B}}\mathbf{u}, \tag{14}$$

where the structure of the dynamic matrix is

$$\bar{\mathbf{A}} = \begin{bmatrix} \bar{\mathbf{A}}_1 & \mathbf{0} & \cdots & \mathbf{0} \\ \mathbf{0} & \bar{\mathbf{A}}_2 & \cdots & \mathbf{0} \\ \cdots & \cdots & \cdots & \cdots \\ \mathbf{0} & \mathbf{0} & \cdots & \bar{\mathbf{A}}_n \end{bmatrix} \tag{15}$$

with

$$\bar{\mathbf{A}}_i = \begin{bmatrix} -(\bar{C}_i - \mathrm{i}\omega\bar{G}_i) & -(\bar{K}_i - \mathrm{i}\omega\bar{C}_{ri}) \\ 1 & 0 \end{bmatrix}. \tag{16}$$

The transformation matrix to obtain the state variables $\bar{\bar{\mathbf{z}}}$ from $\bar{\mathbf{z}}$ is the matrix of the eigenvectors of matrix $\bar{\mathbf{A}}$. If $\mathbf{U}_1 = \text{eigenvectors}\,(\bar{\mathbf{A}})$, it follows that

$$\bar{\bar{\mathbf{z}}} = \mathbf{U}_1\bar{\mathbf{z}} = \mathbf{U}_1\mathbf{U}^{-1}\mathbf{z}. \tag{17}$$

The input gain matrix $\bar{\mathbf{B}}$ is then

$$\bar{\mathbf{B}} = \mathbf{U}_1\mathbf{U}^{-1}\mathbf{B}. \tag{18}$$

In the case of the homogeneous equations the state variables $\bar{\bar{z}}_i$, are directly the modal co-ordinates η_i and the related modal velocities, while in the case when input vector $\mathbf{u}$ is present things are more complicated. If $\bar{\bar{z}}_i$ were the modal co-ordinates and velocities, the structure of equation (14) with the dynamic matrix expressed by equations (15) and (16) would imply that the rows with even order of the input gain matrix do vanish. This, however, is not the case and cannot be expected, as the uncoupling is performed in the state space and no immediate interpretation of the modal state variables in terms of modal co-ordinates and velocities is possible. What is still possible is to assume that the elements in even positions of vector $\bar{\bar{\mathbf{z}}}$ are the modal co-ordinates η, but the elements in odd positions

are the modal velocities minus the corresponding element in the even position of vector $\bar{\mathbf{B}}\mathbf{u}$. Operating in this way, the modal forces in equation (11) can be expressed as

$$\bar{\mathbf{f}}_i(t) = (\bar{\mathbf{B}}\mathbf{u})_{(2i-1)} - \mathrm{i}\omega\bar{G}_i(\bar{\mathbf{B}}\mathbf{u})_{(2i)} + \frac{\mathrm{d}(\bar{\mathbf{B}}\mathbf{u})_{(2i)}}{\mathrm{d}t}. \tag{19}$$

Equation (20) can then be used to compute the modal forces due to unbalances or the modal control forces due to active devices.

4. EQUIVALENT VISCOUS DAMPING

The damping properties of rotors, as far as the rotating damping is concerned, are often modelled using the so-called structural or hysteretic damping model. It is essentially based on the definition of a complex stiffness (or a complex Young's modulus when working at the level of material properties) and on the assumption that the phase lag between the stresses and the strains in structural materials is essentially constant and independent of the frequency.

It is also well known that the hysteretic damping model has some severe drawbacks, namely it is unsuitable for systems subjected to non-harmonic (or, better, non-periodic) forcing functions [10] and overestimates damping in low-frequency motion. In the case of rotors this is particularly severe when dealing with rotating damping in almost-synchronous whirling, when the frequency at which the hysteresis cycle is gone through is very low. A practical difficulty in implementing the model is obtaining the numerical values for the relevant parameters, namely the loss factor or the in-quadrature modulus of the material (usually the former is used for low-damping materials, while the second one is mostly used for high-damping ones). Very often analysts resort to values taken from the literature or obtained through experimental testing, taking a suitable allowance for the large uncertainties involved.

The concept of hysteretic damping has been extended also to the rotordynamics fields, with the usual distinction between rotating and non-rotating damping [1, 11]. The synchronous response of systems with hysteretic damping and even with mixed hysteretic and viscous damping properties can thus be computed, as well as the response to non-synchronous excitation and the threshold of stability.

The main limitation of the hysteretic damping model is its strict limitation to the frequency domain computation. Its unsuitability to numerical time domain simulation is a severe drawback not only for its extension to non-linear systems, but also in general for all cases in which time domain modelling is increasingly applied. The possibility of applying the procedure seen above, in which the equations of motion are uncoupled and reduced to those of many single-degrees-of-freedom rotors (in complex co-ordinates) is thus particularly interesting; it allows uncoupling and at the same time it yields a model in which the damping is of the viscous type. A sort of equivalent modal viscous damping is obtained, which is equivalent in the sense that it yields the same complex eigenvalues as the original system.

The study of the dynamic behaviour of the rotor can thus be performed in the time domain, both by integrating the uncoupled systems or even by recombining the modes to obtain the equivalent viscous rotating and non-rotating damping matrices.

The solution for the free circular whirling of a general multi-degrees-of-freedom rotor is of the type

$$\mathbf{q} = \mathbf{q}_0\,\mathrm{e}^{\mathrm{i}st} \quad \text{or} \quad \mathbf{z} = \mathbf{z}_0\,\mathrm{e}^{\mathrm{i}st} \tag{20}$$

depending on whether the equation is written in the configuration or in the state space.

The equations of motion for free circular whirling of an axisymmetrical rotor with mixed (i.e., viscous and hysteretic) damping can thus be written in the frequency domain as

$$(s^2\mathbf{M} + s\mathbf{C} - \mathrm{i}\omega s\mathbf{G} + \mathbf{K} + \mathbf{K}_\omega\omega^2 - \mathrm{i}\omega\mathbf{C}_r \pm \mathbf{K}_n'' \pm \mathbf{K}_r'')\mathbf{q}_0 = \mathbf{0} \tag{21}$$

with reference to the configuration space. By resorting to a state-space approach, the frequency domain equation is

$$(s\mathbf{I} - \mathbf{A})\mathbf{z}_0 = \mathbf{0}, \tag{22}$$

where

$$\mathbf{A} = \begin{bmatrix} -\mathbf{M}^{-1}(\mathbf{C} - \mathrm{i}\omega\mathbf{G}) & -\mathbf{M}^{-1}(\mathbf{K} + \mathbf{K}_\omega\omega^2 - \mathrm{i}\omega\mathbf{C}_r \pm \mathbf{K}_n'' \pm \mathbf{K}_r'') \\ \mathbf{I} & \mathbf{0} \end{bmatrix}. \tag{23}$$

Matrices $\mathbf{K}''$ are the imaginary parts of the complex stiffness matrices related to the stator and the rotor, and the double signs are stated following this simple rule:

- The term in $\mathbf{K}_n''$ is positive for forward whirling ($\Im(s) > 0$) and negative for backward whirling ($\Im(s) < 0$).
- The term in $\mathbf{K}_r''$ is positive for subcritical forward whirling ($\Im(s) > \omega$) and negative for supercritical forward whirling ($0 < \Im(s) < \omega$) and for backward whirling ($\Im(s) < 0$).

The computation must then proceed by solving three eigenproblems (with two positive signs, with positive and negative signs and with two negative signs) and then choosing among the computed modes those which obey the above-mentioned rules [1, 11]. An eigenvector matrix and a set of eigenvalues is thus obtained and the procedure can proceed following the same rules as seen above for systems with viscous damping.

Note that equations (21) and (23) are approximated and their accuracy increases with decreasing hysteretic damping and increasing value of the difference between the whirl and the spin speeds (abs$(\Im(s) - \omega)$). This would preclude the use of this model for synchronous whirling, but this can be circumvented by noting that in that condition rotating damping plays no role in the dynamic behaviour of the rotor and matrix $\mathbf{K}_r''$ can be altogether neglected.

5. EXAMPLES

5.1. JEFFCOTT ROTOR WITH HYSTERETIC DAMPING

The simplest model for the flexural behaviour of rotors is the so-called Jeffcott rotor, i.e., a point mass P, with mass m, attached to a massless shaft of stiffness k (Figure 1). Point mass P may lie at a small distance from the geometrical centre C of the shaft, giving way to static unbalance with eccentricity ε.

Using the complex co-ordinate $z = x + iy$, the frequency domain equation of a Jeffcott rotor with hysteretic damping, subjected to a non-synchronous circular forcing function $f = f_0\,\mathrm{e}^{\mathrm{i}\lambda t}$ with whirl frequency λ, is

$$[-m\lambda^2 + k + \mathrm{i}(\pm k_n'' \pm k_r'')]\,z_0 = f_0. \tag{24}$$

The eccentricity causes a synchronous forcing function $f = m\varepsilon\omega^2\,\mathrm{e}^{\mathrm{i}\omega t}$.

Note that while this equation is approximated when studying the free whirling of the system (the whirl frequency being a complex quantity), in the study of the forced response λ is the (real) frequency of a forced motion and then the equation contains no

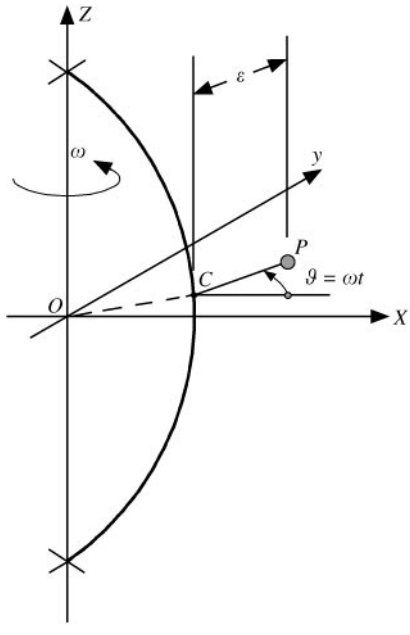

Figure 1. Sketch of a Jeffcott rotor. Point P, with mass m, is attached to a massless shaft with stiffness k with an eccentricity ε.

approximations. The same holds for the unbalance response in which ω is substituted for λ, with the added consideration that in synchronous whirling the term in k_r'' must be omitted.

By introducing the natural frequency of the undamped system, and normalizing with it both the whirl and the spin speed,

$$\lambda^* = \frac{\lambda}{\lambda_0} = \frac{\lambda}{\sqrt{k/m}}, \quad s^* = \frac{s}{\lambda_0} = -\frac{s}{\sqrt{k/m}}, \quad \omega^* = \frac{\omega}{\lambda_0} = -\frac{\omega}{\sqrt{k/m}} \tag{25}$$

the dynamic matrix of the system is simply

$$\mathbf{A} = \begin{bmatrix} 0 & -(1 \pm \mathrm{i}\eta_n \pm \mathrm{i}\eta_r) \\ 1 & 0 \end{bmatrix}, \tag{26}$$

where $\eta_i = k_i''/k$.

The solutions of the eigenproblem yielding the free whirling frequencies of the damped system are the following:

- Case with two positive signs

$$s^* = \pm\left(-\sqrt{\frac{-1 + \sqrt{1 + (\eta_n + \eta_r)^2}}{2}} + \mathrm{i}\sqrt{\frac{1 + \sqrt{1 + (\eta_n + \eta_r)^2}}{2}}\right). \tag{27}$$

- Case with two negative signs

$$s^* = \pm\left(\sqrt{\frac{-1 + \sqrt{1 + (\eta_n + \eta_r)^2}}{2}} + \mathrm{i}\sqrt{\frac{1 + \sqrt{1 + (\eta_n + \eta_r)^2}}{2}}\right). \tag{28}$$

- Case with a positive and negative sign. Here there are two subcases:

(1) $\eta_n > \eta_r$

$$s^* = \pm\left(-\sqrt{\frac{-1+\sqrt{1+(\eta_n-\eta_r)^2}}{2}} + \mathrm{i}\sqrt{\frac{1+\sqrt{1+(\eta_n-\eta_r)^2}}{2}}\right). \tag{29}$$

(2) $\eta_n < \eta_r$

$$s^* = \pm\left(\sqrt{\frac{-1+\sqrt{1+(\eta_n-\eta_r)^2}}{2}} + \mathrm{i}\sqrt{\frac{1+\sqrt{1+(\eta_n-\eta_r)^2}}{2}}\right). \tag{30}$$

For the choice among the solutions obtained above, the discriminating factor is whether the speed is smaller or higher than the critical speed, or better, than the imaginary part of s.

In the first cases ($\omega^* < \sqrt{[1+\sqrt{1+(\eta_n-\eta_r)^2}]/2}$), the two solutions are equation (28) with (+) and equation (28) with (−). Equation (14) can be used to compute the modal parameters, obtaining

$$\begin{aligned} \bar{K} &= \tfrac{k}{m}\sqrt{1+(\eta_n+\eta_r)^2} \approx \tfrac{k}{m}, & \bar{G} &= 0, \\ \bar{C} &= \sqrt{\tfrac{2k}{m}}\ \sqrt{-1+\sqrt{1+(\eta_n+\eta_r)^2}} \approx \tfrac{k}{m\lambda_0}(\eta_n+\eta_r), & \bar{C}_r &= 0. \end{aligned} \tag{31}$$

The approximated values have been obtained assuming that the loss factor is small when compared with unity, as is usually the case.

In the second case ($\omega^* > \sqrt{[1+\sqrt{1+(\eta_n-\eta_r)^2}]/2}$), two subcases must be distinguished:

- If $\eta_n > \eta_r$ the two solutions are equation (29) with (+) and equation (28) with (−). Equation (14) can be used to compute the modal parameters, but no closed-form solution is reported here owing to the complexity of the result. Note that in this case the gyroscopic term $\bar{G}$ is not exactly zero, although being small. This may appear strange, as by definition the Jeffcott rotor has no gyroscopic effect, but it must be kept in mind that in this context the gyroscopic term has the aim of accounting for different values of the whirl frequency in forward and backward whirlings as in a Jeffcott rotor with viscous damping they are equal while in a supercritical rotor whereas with hysteretic damping they differ from each other, the only way being to assign an equivalent gyroscopic term to the systems. If damping is small, this term vanishes, and the modal parameters are

$$\begin{aligned} \bar{K} &\approx \tfrac{k}{m}, & \bar{G} &\approx 0, \\ \bar{C} &\approx \tfrac{k\eta_n}{m\lambda_0}, & \bar{C}_r &\approx \tfrac{k\eta_r}{m\omega}. \end{aligned} \tag{32}$$

- If $\eta_n < \eta_r$ the two solutions are equation (30) with (+) and equation (29) with (−). The solution for forward whirling has a positive real part and hence is unstable, as it is well known. Again, the exact expression of the modal parameters is too complex to be reported here. The modal parameters for small damping are

$$\begin{aligned} \bar{K} &\approx \tfrac{k}{m}, & \bar{G} &\approx 0, \\ \bar{C} &\approx -\tfrac{k\eta_n}{m\lambda_0}, & \bar{C}_r &\approx -\tfrac{k\eta_r}{m\omega}. \end{aligned} \tag{33}$$

The modal parameters for a Jeffcott rotor with $\eta_n = 0{\cdot}08$ and $\eta_r = 0{\cdot}04$ are reported in Figure 2. Note that in the above equations to distinguish whether the system works in the

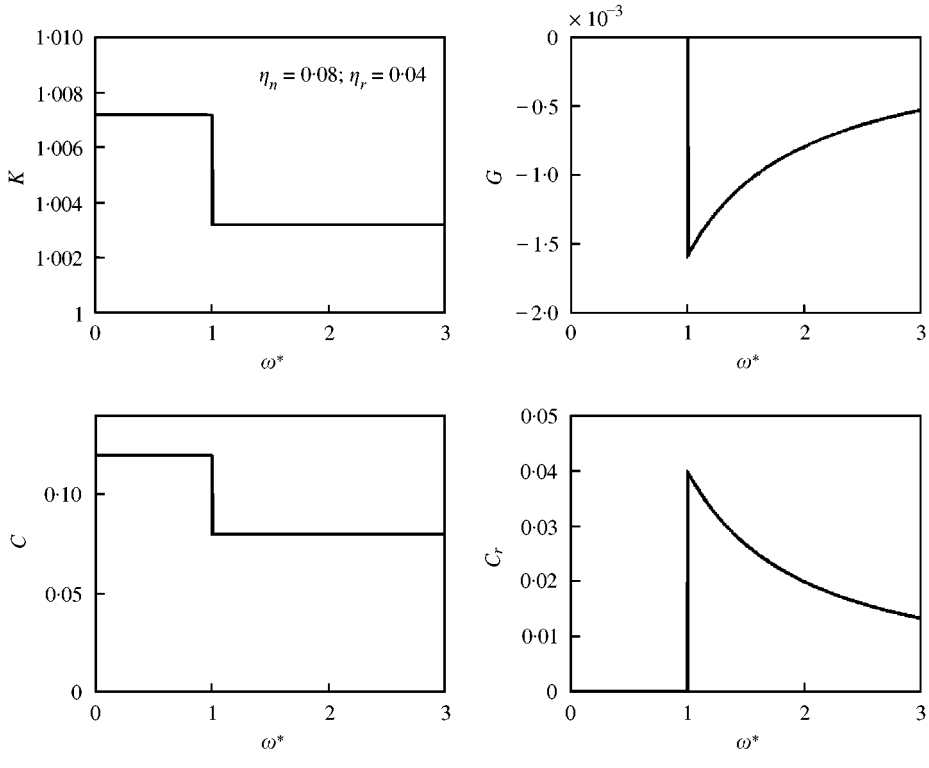

Figure 2. Modal parameters for a Jeffcott rotor with $\eta_n = 0{\cdot}08$ and $\eta_r = 0{\cdot}04$.

subcritical region a check of the type $\omega^* < \sqrt{[1 + \sqrt{1 + (\eta_n - \eta_r)^2}]/2)}$ was performed. There is no reason not to use a different criterion: $\omega^* < \sqrt{[1 + \sqrt{1 + (\eta_n + \eta_r)^2}]/2)}$. This introduces an ambiguity in the procedure, which is, however, only an apparent one: owing to the smallness of hysteretic damping, the two values are very close to each other (in the numerical example they are $\omega^* < 1{\cdot}0002$ and $1{\cdot}0018$); moreover, it has little meaning to investigate what happens between these values, as the very model of hysteretic damping loses meaning when close to the condition $\Im(s^*) \approx \omega^*$.

The unbalance response of the same system is reported in Figure 3. The zone close to the peak has been enlarged, to show that in the vicinity of the critical speed the two models used yield different results, as expected. This is, however, not a severe drawback: as will be stated later this approach is not very convenient when dealing with the unbalance response, and the present case is not typical, as it contains quite a large hysteretic damping (particularly where the rotating damping is concerned).

The responses to harmonic excitation for the two cases of subcritical operation with $\omega^* = 0{\cdot}5$, and supercritical operation with $\omega^* = 1{\cdot}5$, are shown in Figure 4. The differences between the solution computed using the hysteretic damping model and that obtained with the equivalent viscous damping are so small that it cannot be seen in the Figure.

As a final check plots of the type of that of Figure 4 were obtained with varying ω^*, and the difference between the peak amplitudes obtained using the two different models was computed. The relative error is plotted in Figure 5 as a function of ω^*. Note that in the subcritical range the error is vanishingly small and in the supercritical range it is very small

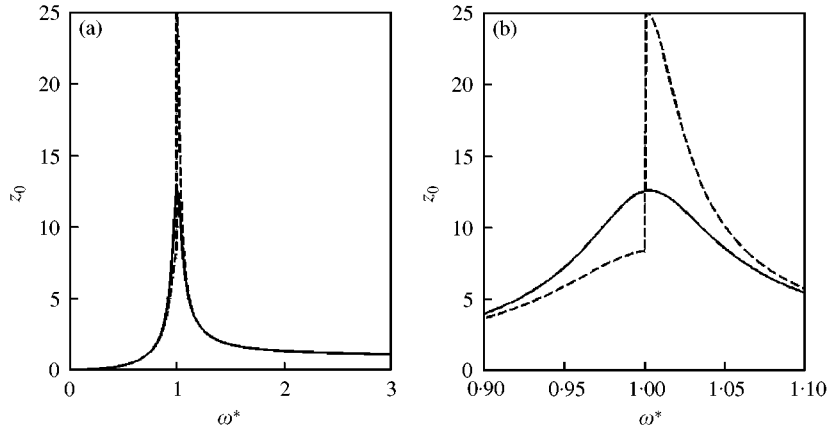

Figure 3. (a) Unbalance response for a Jeffcott rotor with $\eta_n = 0{\cdot}08$ and $\eta_r = 0{\cdot}04$. Solution computed using the hysteretic damping model: full line; solution with the equivalent viscous damping: dashed line. (b) Same as (a), for a speed range close to the critical speed.

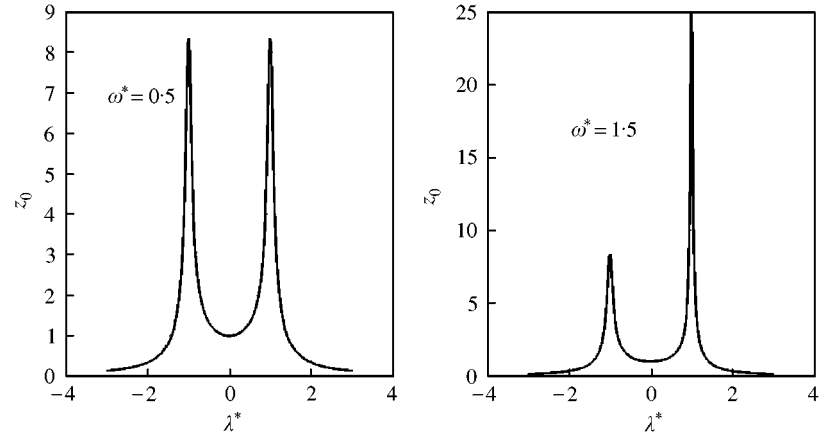

Figure 4. Response to a harmonic excitation for the two cases of subcritical operation with $\omega/\lambda_n = 0{\cdot}5$ and supercritical operation with $\omega/\lambda_n = 1{\cdot}5$. The solution computed using the hysteretic damping model and that obtained with the equivalent viscous damping are completely superimposed.

(of the order of 0·1%). At the critical speed a large error is present, and the response is doubled. Note that this very high error, like the error in similar conditions found in Figure 3, is linked with the particular data used for the example, and that it is usually far smaller. Note also that the speed range in which a large error is found is very narrow.

5.2. THE STODOLA–GREEN ROTOR

Consider as a second example, the so-called Stodola–Green rotor: a disc attached at the end of a prismatic cantilever beam (Figure 6). It can be modelled as a rotor with two complex (four real) degrees of freedom: by neglecting damping and assuming that the only forcing function is due to the static unbalance of the disc, the equation of motion is

$$\mathbf{M}\ddot{\mathbf{q}} - \mathrm{i}\omega\mathbf{G}\dot{\mathbf{q}} + \mathbf{K}\mathbf{q} = \omega^2 \mathbf{f}_r \mathrm{e}^{\mathrm{i}\omega t}, \tag{34}$$

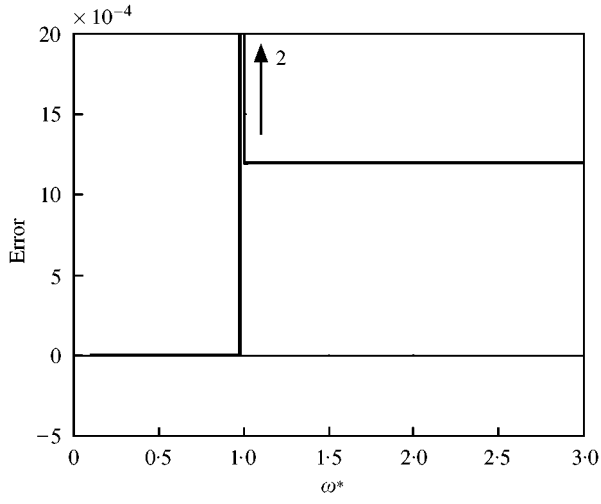

Figure 5. Relative error between the peak amplitude of the frequency response of a Jeffcott rotor with $\eta_n = 0{\cdot}08$ and $\eta_r = 0{\cdot}04$, computed using the hysteretic damping and the equivalent viscous damping models.

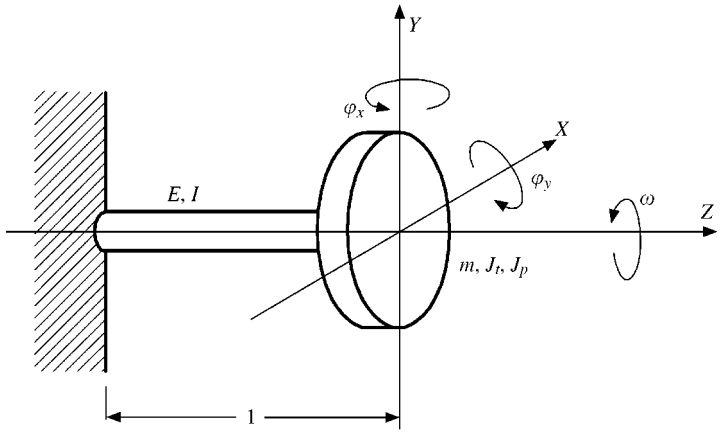

Figure 6. Sketch of a Stodola–Green rotor: a disc, with mass m and moments of inertia J_t and J_p, attached at the end of a prismatic massless cantilever shaft.

where the relevant vectors and matrices are

$$\mathbf{q} = \begin{Bmatrix} x + \mathrm{i}y \\ \phi_y - \mathrm{i}\phi_x \end{Bmatrix}, \quad \mathbf{f}_r = \begin{Bmatrix} m\varepsilon \\ 0 \end{Bmatrix},$$

$$\mathbf{M} = \begin{bmatrix} m & 0 \\ 0 & J_t \end{bmatrix}, \quad \mathbf{G} = \begin{bmatrix} 0 & 0 \\ 0 & J_p \end{bmatrix}, \quad \mathbf{K} = \frac{EI}{l^3} \begin{bmatrix} 12 & -6l \\ -6l & 4l^2 \end{bmatrix}, \tag{35}$$

where E, I and l are, respectively, the Young's modulus of the material, the area moment of inertia of the cross-section and the length of the shaft. The equation of motion can be written in non-dimensional form as

$$\begin{bmatrix} 1 & 0 \\ 0 & \beta \end{bmatrix} \begin{Bmatrix} \dfrac{\ddot{z}}{\varepsilon\lambda_0^2} \\ \dfrac{l\ddot{\phi}}{\varepsilon\lambda_0^2} \end{Bmatrix} - \mathrm{i}\omega^* \begin{bmatrix} 0 & 0 \\ 0 & \alpha\beta \end{bmatrix} \begin{Bmatrix} \dfrac{\dot{z}}{\varepsilon\lambda_0} \\ \dfrac{l\dot{\phi}}{\varepsilon\lambda_0} \end{Bmatrix} + \begin{bmatrix} 4 & -2 \\ -2 & \frac{4}{3} \end{bmatrix} \begin{Bmatrix} \dfrac{z}{\varepsilon} \\ \dfrac{l\phi}{\varepsilon} \end{Bmatrix} = \begin{Bmatrix} \omega^{*2} \\ 0 \end{Bmatrix} \tag{36}$$

by introducing parameters

$$\alpha = \frac{J_p}{J_t}, \quad \beta = \frac{J_t}{ml^2} = \left(\frac{r_t}{l}\right)^2, \tag{37}$$

where $r_t = \sqrt{J_t/m}$ is the radius of inertia of the disc corresponding to the moment of inertia J_t. The non-dimensional whirl and spin speed are defined as

$$\lambda^* = \frac{\lambda}{\lambda_0}, \quad \omega^* = \frac{\omega}{\lambda_0}, \tag{38}$$

where

$$\lambda_0 = \sqrt{\frac{3EI}{ml^3}} \tag{39}$$

is the natural frequency at standstill when the disc at the tip of the beam has negligible moments of inertia (parameter $\beta \to 0$). Assuming a solution of the type

$$\begin{Bmatrix} z \\ l\phi \end{Bmatrix} = \begin{Bmatrix} z_0 \\ l\phi_0 \end{Bmatrix} e^{i\lambda t} \tag{40}$$

the equation for free whirling is

$$\left\{ -\lambda^{*2} \begin{bmatrix} 1 & 0 \\ 0 & \beta \end{bmatrix} + \omega^*\lambda^* \begin{bmatrix} 0 & 0 \\ 0 & \alpha\beta \end{bmatrix} + \begin{bmatrix} 4 & -2 \\ -2 & \frac{4}{3} \end{bmatrix} \right\} \begin{Bmatrix} z_0 \\ l\phi_0 \end{Bmatrix} = \mathbf{0}. \tag{41}$$

The non-dimensional whirl frequencies of the system depend on two parameters, namely ratio β, assessing the importance of the transverse moment of inertia with respect to the mass, and the product $\alpha\omega^*$, assessing the importance of the gyroscopic effect. If $\beta \to 0$ the behaviour of the rotor tends to that of the Jeffcott model; the non-dimensional frequency of the first mode tends to 1 and does not depend on the speed, while the frequency of the second mode tends to infinity (there is only one mode). With increasing β the effect of the speed increases and the frequency of the second mode (both forward and backward) is increasingly lower.

The non-dimensional Campbell diagrams for the cases with $\beta = 0{\cdot}1$ and 1 (a very high value, corresponding to a very large disc, with a radius of inertia related to J_t equal to the length of the beam) are reported in Figure 7. The full lines refer to the non-modal solution and the modal solution obtained with modal parameters obtained for each value of the speed; the dashed lines refer to a modal solution obtained with fixed modal parameters.

From the Figure it is clear that the results obtained using the modal procedure with fixed parameters are unacceptable, particularly in the case of the higher value of β and for the forward whirl branches of the plot.

The modal parameters K and G are reported in Figure 8.

The computation of the unbalance response is straightforward. Assuming a solution of the type

$$\begin{Bmatrix} z \\ l\phi \end{Bmatrix} = \begin{Bmatrix} z_0 \\ l\phi_0 \end{Bmatrix} e^{i\omega t}, \tag{42}$$

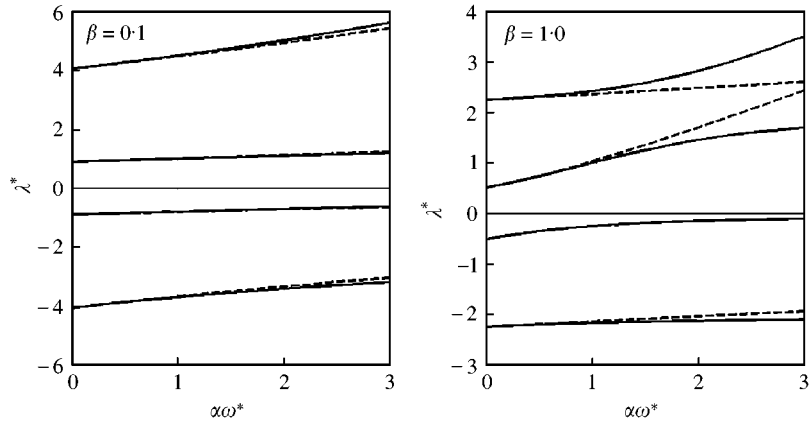

Figure 7. Non-dimensional Campbell diagrams for the Stodola–Green rotor with $\beta = 0{\cdot}1$ and 1. The —— lines refer to the non-modal solution and the modal solution obtained with modal parameters obtained for each value of the speed: the – – – lines refer to a modal solution obtained with fixed modal parameters.

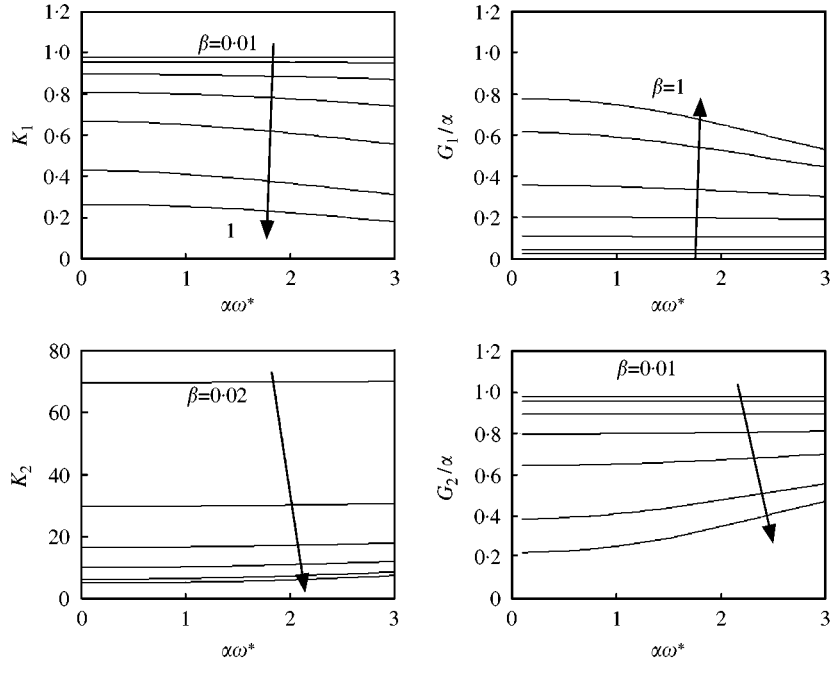

Figure 8. Modal stiffness and gyroscopic parameter K and G as function of the non-dimensional speed $\alpha\omega^*$ for the two modes. The various curves refer to $\beta = 0{\cdot}01$, 0·02, 0·05, 0·1, 0·2, 0·5 and 1.

the equation yielding the response to static unbalance with eccentricity ε is

$$\left\{ -\omega^{*2}\begin{bmatrix} 1 & 0 \\ 0 & \beta(1+\alpha) \end{bmatrix} + \begin{bmatrix} 4 & -2 \\ -2 & \frac{4}{3} \end{bmatrix} \right\} \begin{Bmatrix} \dfrac{z_0}{\varepsilon} \\ \dfrac{l\phi_0}{\varepsilon} \end{Bmatrix} = \begin{Bmatrix} \omega^{*2} \\ 0 \end{Bmatrix}. \tag{43}$$

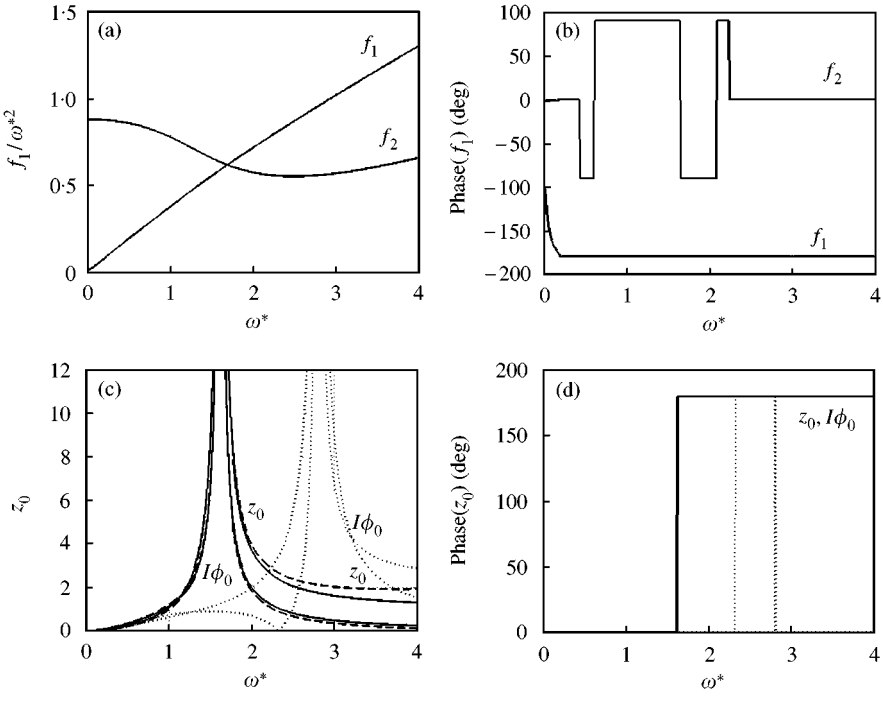

Figure 9. Unbalance response of a Stodola–Green rotor with $\alpha = 1{\cdot}6$ and $\beta = 1$. (a), (b). Modal unbalance forces (amplitude and phase) acting on the two uncoupled modal gyroscopic systems (c), (d). Amplitude and phase of the unbalance response computed using the original equations and modal equations with two modes (superimposed to each other, —— lines), response computed using a single mode (– – – lines) and using two modes, but uncoupling the equation of motion using the modal co-ordinates in the configuration space (equation (3)) and neglecting the out-of diagonal terms of the gyroscopic matrix (····· lines).

The non-dimensional unbalance response of a Stodola–Green rotor with $\alpha = 1{\cdot}6$ and $\beta = 1$ is reported in amplitude and phase in Figure 9(c) and 9(d), full lines. The system has a single critical speed, $\omega^*_{cr} = 1{\cdot}62$. The other critical speed is imaginary, and its modulus is 0·9202.

The non-dimensional modal unbalance forces acting on the two uncoupled modal gyroscopic systems with the speed-dependent modal parameters shown in Figure 9, normalized by dividing them by $\varepsilon\omega^{*2}$, are reported in amplitude and phase in Figure 9(a) and 9(b). The unbalance response, computed using the modal equations (with two modes) and then transforming the results to physical co-ordinates is completely superimposed to the non-modal result, as expected. The response computed using a single mode (dashed lines) is quite close to the correct response, at least around the zone of the peak. As the absolute value of the imaginary critical speed is not much higher (actually it is lower) than the critical speed, the response computed using a single mode cannot be expected to be very close to the correct one [12].

The response computed using two modes, but uncoupling the equations of motion using the modal co-ordinates in the configuration space (equation (3)) and neglecting the out-of diagonal terms of the gyroscopic matrix (dotted lines), leads to very large errors and shows that this way of proceeding cannot be followed, at least for highly gyroscopic systems like the present one.

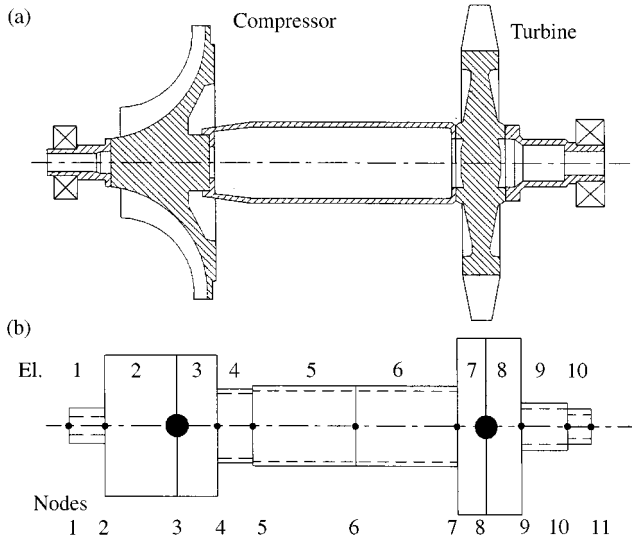

Figure 10. Sketch (a) and FEM model (b) of the rotor of a small gas turbine used as Example 3.

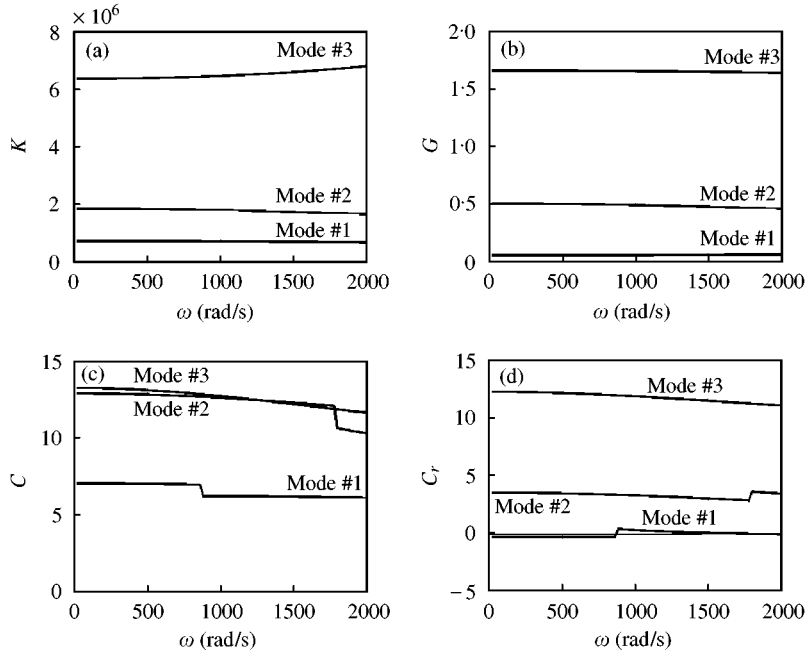

Figure 11. Modal parameters for the first 3 modes of the rotor used as example 3, plotted against the spin speed ω.

5.3. ROTOR OF A SMALL GAS TURBINE

Consider the rotor of a small gas turbine described as Example 4.3 in reference [1, p. 339] (Figure 10). Assume that the stiffness of the bearings is 20 MN/m and that the loss factors of the supports and of the shaft material are, respectively, 0·01 and 0·004. The

system is modelled using 22 degrees of freedom, which are reduced to 8 (translations at nodes 1, 3, 4, 6, 7, 8, 9 and 11) through Guyan reduction.

The modal parameters for the first three modes (gyroscopic effect, stiffness, total damping and rotating damping; the modal mass has a unit value) are plotted as functions of the speed in Figure 11. Note that the total damping and the rotating damping are equivalent viscous damping coefficient for hysteretic damping; they change abruptly at the critical speeds, as could be expected. In this case the equivalent viscous rotating damping for the first mode is very small (in the first mode the rotor behaves almost as a rigid body and its damping has little influence on the dynamic behaviour) and is negative at some speeds.

The response to a unit eccentricity of the compressor wheel is plotted as a function of speed in Figure 12. Owing to the small damping, the two peaks corresponding to the crossing of the two critical speeds are quite high. The response computed using the non-modal procedure and the hysteretic damping model, is reported together with the response computed using the present modal approach and the equivalent viscous damping (full lines). The response was also computed using a reduced number of modes (dashed lines). The computation performed using only the first mode (first forward and backward modes) is quite close to the correct one at speeds not much in excess of the first critical speed, but then the errors become unacceptable. At higher speeds at least two modes must be used: the curves obtained using 2, 3 and 8 modes are completely superimposed in the whole field of interest.

5.4. ROTOR ON ACTIVE BEARINGS

Consider the same rotor studied in the previous example, but assume that it is supported by two active bearings located at nodes 1 and 11, with perfectly co-located sensors and

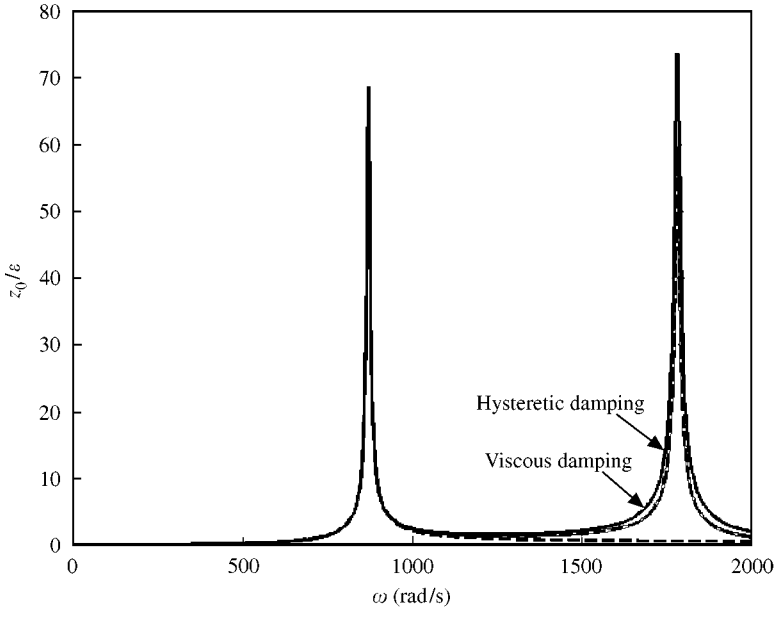

Figure 12. Unbalance response at the centre of gravity of the compressor wheel (node 3) for a unit eccentricity in the same point. Response computed using the complete model (hysteretic damping) and the present modal approach (all modes, viscous damping). The – – – line refers to a response computed using only the first forward and backward modes.

actuators. Neglect the open-loop negative stiffness of the electromagnetic actuators and assumed ideal sensors, actuators and power amplifiers.

The system has 8 degrees of freedom (after Guyan reduction) and the control forces are applied on two nodes: matrix $\mathbf{T}_n$ to be introduced into equation (9) has then eight rows and two columns, and contains all zeros except for the elements 1,1 and 2,8 which have a unit value:

$$\mathbf{T}_n = \begin{bmatrix} 1 & 0 & 0 & 0 & 0 & 0 & 0 & 0 \\ 0 & 0 & 0 & 0 & 0 & 0 & 0 & 1 \end{bmatrix}^{\mathrm{T}}. \tag{44}$$

Vector $\mathbf{f}_n = [f_{c1}, f_{c2}]^{\mathrm{T}}$ has two elements, namely the forces supplied by the two actuators. Using the complex notation, they are complex numbers, with the real part being the x component of the force and the imaginary part being the y component.

Assuming a simple ideal, decentralized, PD active control implemented through direct measurement of the displacements and velocities at the sensor locations, it is possible to write an output vector $\mathbf{y} = [\dot{q}_1, \dot{q}_8, q_1, q_8]^{\mathrm{T}}$ and an output gain matric $\mathbf{C}$ with four rows and 16 columns, in which all elements are equal to zero except for elements 1,1: 2,8: 3,9 and 4,16 which have a unit value.

The control gain matrix is then defined by the relationship

$$\mathbf{u}_c = \begin{Bmatrix} f_{c1} \\ f_{c2} \end{Bmatrix} = -\mathbf{G}_c\mathbf{y} = -\begin{bmatrix} k_{d1} & 0 & k_{p1} & 0 \\ 0 & k_{d2} & 0 & k_{p2} \end{bmatrix}\mathbf{y}, \tag{45}$$

where the proportional gains k_p and the derivative gains k_d contain all the gains from the sensors to the actuators.

By closing the loop in this way, the control input vector can be written in the form

$$\mathbf{u}_c = -\mathbf{G}_c\mathbf{C}\mathbf{z}. \tag{46}$$

The closed-loop dynamic matrix of the system is then

$$\mathbf{A}_{cl} = \mathbf{A}_{ol} - \mathbf{B}\mathbf{G}_c\mathbf{C}. \tag{47}$$

By using the matrix of the complex right eigenvectors $\mathbf{U}$ of the open-loop dynamic matrix $\mathbf{A}_{ol}$, the closed-loop dynamic matrix can be written in modal form

$$\bar{\mathbf{A}}_{cl} = \mathbf{U}^{-1}\mathbf{A}_{ol}\mathbf{U} - \mathbf{U}^{-1}\mathbf{B}\mathbf{G}_c\mathbf{C}\mathbf{U}. \tag{48}$$

Note that the modal closed-loop dynamic matrix is not diagonal, even if the open loop is, because the control systems couples the various modes. This is unavoidable, since the eigenvectors of the open-loop system and those of the closed-loop one are different.

As usual with modal control, it is possible to use a reduced order model to design the controller, i.e., to take into account only a reduced number of eigenvectors in performing the modal transformation in equation (48). To evaluate the errors linked with the use of reduced order models in the present case, assume the following gain matrix:

$$\mathbf{G}_c = 10^3 \begin{bmatrix} 4 & 0 & 2000 & 0 \\ 0 & 4 & 0 & 2000 \end{bmatrix} \tag{49}$$

and compute the first six eigenvalues at a speed $\omega = 2000$ rad/s using the complete model and the reduced order one. The results are shown in Table 1. Note that the open-loop model is unstable; the second forward mode has a positive real part. This could be expected, as it is typical of free 'long rotors' (rotors with $J_p < J_t$) [10, 13]. The closed-loop system is stable, owing to the high derivative gain and, above all, to the fact that there is a perfect co-location between sensors and actuators, The reduced order model in which only the first four modes

TABLE 1

First six complex eigenvalues (three forward and three backward modes) for the open- and the closed-loop systems. The computation of the eigenvalues of the closed-loop rotor has been performed using the complete modal system (16 modes) and with two reduced order models (four modes and six modes)

		Closed loop		
Mode	Open loop	16 modes (full)	Four modes	Six modes
I BWD	0	$-42\ -148i$	$-41\ -150i$	$-41\ -150i$
I FWD	0	$-94\ +296i$	$-98\ +298i$	$-95\ +297i$
II BWD	0	$-92\ -296i$	$-98\ -298i$	$-94\ -297i$
II FWD	$0{\cdot}4 + 981i$	$-303\ +1135i$	$-309\ +1125i$	$-309\ +1125i$
III BWD	$-3{\cdot}6\ -1117i$	$-56\ -1129i$	—	$-57\ -1128i$
III FWD	$-3{\cdot}7\ +4526i$	$-192\ +4552i$	—	$-194\ +4538i$

have been considered gives a set of eigenvalues which are almost coincident with the first four eigenvalues of the complete model. If more than four natural frequencies are required, it is necessary to resort to a model containing more modes: a reduced model of order 6 allows the fifth and sixth natural frequency to be obtained with very good precision, while refining the values of the first four.

6. CONCLUSIONS

A new way of uncoupling the equations of motion typical for rotordynamics has been introduced. It allows the n equations of motion ($2n$ if the model is written with reference to the state space) of a rotor with n complex degrees of freedom to be split into n uncoupled equations, i.e., a rotor with n degrees of freedom is split into n single-degree-of-freedom gyroscopic systems. More conventionally, it can be split into $2n$ uncoupled systems written in the state space, but in the latter case it is impossible to distinguish between modal stiffness and modal gyroscopic term.

In the case of hysteretic type of damping, the uncoupled gyroscopic systems are provided with an equivalent viscous damping, where the term "equivalent" means that it leads to the same natural frequency and decay rate. It has then the same meaning as is used for constant viscous equivalent damping, i.e., a viscous damping leading to the same amplitude in resonant conditions.

The following points must be kept in mind:

- Transformation (10) needed to obtain the uncoupled modal system in the space state is straightforward and does not need any more work than that needed for the computation of the Campbell diagram and of the related eigenvectors.
- Even if only a reduced number of modes is required, all eigenvectors must be obtained in order to invert the eigenvectors matrices, needed to compute the modal input gain matrix. In case of a large number of degrees of freedom, the use of Guyan reduction can be important for reducing the amount of computational work.
- When computing the unbalance response, the modal uncoupling does not provide any simplification of the computation. On the contrary, it requires the computations of the

eigenvalues and the eigenvectors at the various speeds, instead of the mere solution of a set of linear equations.

- When computing the response of the system at a fixed speed a computational advantage is present on the contrary, since a single eigenproblem has to be solved. and then the response (at varying excitation frequency) can be computed from uncoupled equations. For this task transformation (17) is not really needed as transformation (10) is sufficient.
- The modal uncoupling presented here can be very useful in the design of the control system for actively controlled rotors. Even if the control system couples the various modes, reduced order models can be devised simply by taking into account a reduced number of eigenvectors. The results are approximated, owing to the presence of some spillover, but a numerical example has shown that the approximation obtained is very good. The model used for the design of the controller is speed dependent: if it is impossible to design a fixed parameters controller which behaves satisfactorily in the required speed range, it is possible to resort to gain scheduling by designing a number of controllers adapted to different speeds (see for example reference [14]).

Throughout the whole paper models based on the complex-co-ordinates approach have been used and the rotor has been assumed to be axially symmetrical. This is convenient in order to reduce the complexity of the various formulae, but is not required; the present approach works well even if real co-ordinates are used (with the need of doubling the number of equations and grouping them four by four instead of two by two). Systems which are non-isotropic can thus be studied, using either the standard real co-ordinates approach, or by introducing mean and deviatoric matrices and using complex co-ordinates.

REFERENCES

1. G. GENTA 1998 *Vibration of Structures and Machines*. New York; Springer-Verlag, third edition.
2. G. GENTA 1988 *Journal of Sound and Vibration* **124**, 27–53. Whirling of unsymmetrical rotors, a finite element approach based on complex coordinates.
3. L. MEIROVITCH 1975 *American Society of Mechanical Engineers Journal of Applied Mechanics* **42**, 446–450. *A modal analysis for the response of linear systems.*
4. L. MEIROVITCH 1974 *American Institute of Aeronautics and Astronautics Journal* **12**, 1337–1342. A new method of solution of the eigenvalue problem for gyroscopic systems.
5. D. W. CHILDS 1974 *American Society of Mechanical Engineers Journal of Engineering for Industry* **96**, 659–669. A rotor-fixed modal simulation model for flexible rotating equipment.
6. G. GENTA 1992 *Journal of Sound and Vibration* **155**, 385–402. A fast modal technique for the computation of the Campbell diagram of multi-degrees of freedom rotors.
7. W. GAWRONSKI and J. T. SAWICKI 1997 *Journal of Sound and Vibration* **200**, 543–550. Response errors of non-proportionally lightly damped structures.
8. W. WANG and J. KIRKHOPE 1994 *Journal of Sound and Vibration* **175**, 159–170. New eigensolutions and modal analysis for gyroscopic/rotor systems, Part I: Undamped systems.
9. W. WANG and J. KIRKHOPE 1994 *Journal of Sound and Vibration* **175**, 171–183. New eigensolutions and modal analysis for gyroscopic/rotor systems. Part 2. Perturbation analysis for damped systems.
10. S. H. CRANDALL 1995 in *Nonlinear Dynamics and Stochastic Mechanics* (W. H. Kliemann and N. S. Namachchivaya, editors, 3–44). Boca Raton, FL: CRC Press. Rotordynamics.
11. G. RAMANUJAM and C. W. BERT 1983 *Journal of Sound and Vibration* **88**, 369–420. Whirling and stability of flywheel systems. Part I. Derivation of combined and lumped parameter models. Part II. Comparison of numerical results obtained with combined and lumped parameter models.
12. G. GENTA and F. DE BONA 1991 *Journal of Sound and Vibration* **140**, 129–153. Unbalance response of rotors: a modal approach with some extensions to damped natural systems.
13. G. GENTA, C. DELPRETE and E. BRUSA 1999 *Journal of Sound and Vibration* **227**, 611–645. Some considerations on the basic assumptions in rotordynamics.
14. J. S. SHAMMA and M. ATHANS 1991 *Automatica* **27**, 559–564. Guaranteed properties of gain scheduled control for linear parameter-varying plants.

APPENDIX. A: NOMENCLATURE

$\mathbf{f}$	force vector
i	imaginary unit ($\mathrm{i} = \sqrt{-1}$)
k	stiffness, gain
l	length
m	mass
$\mathbf{q}$	vector of the generalized co-ordinates (complex)
s	eigenvalue, Laplace variable
t	time
$\mathbf{u}$	input vector
$\mathbf{x}$	vector of the generalized co-ordinates (real)
xyz	reference frame
$\mathbf{y}$	output vector
$\mathbf{z}$	state vector
$\mathbf{A}$	dynamic matrix
$\mathbf{B}$	input gain matrix
$\mathbf{C}$	total damping matrix, output gain matrix
E	Young's modulus
$\mathbf{G}$	gyroscopic matrix
$\mathbf{G}_c$	control gain matrix
I	area moment of inertia of the cross-section
J_p	moment of inertia (polar)
J_t	moment of inertia (transversal)
$\mathbf{K}$	stiffness matrix
$\mathbf{K}''$	imaginary part of the stiffness matrix
$\mathbf{K}_\omega$	centrifugal stiffening matrix
$\mathbf{M}$	mass matrix
$\mathbf{T}$	selection matrix
$\mathbf{U}$	matrix or the right eigenvectors
η	loss factor
$\boldsymbol{\eta}$	vector of the modal co-ordinates
λ	whirl speed
ϕ	rotation
ω	spin speed
$^-$	modal matrix or vector

Subscripts

cl	closed loop
d	derivative
n	non-rotating
ol	open loop
p	proportional
r	rotating